This paper is published as part of a *Dalton Transactions* themed issue on:

Emerging Strategies in Catalysis

Guest Edited by Carmen Claver
Universitat Rovira i Virgili, Tarragona

Published in issue 47, 2007 of *Dalton Transactions*

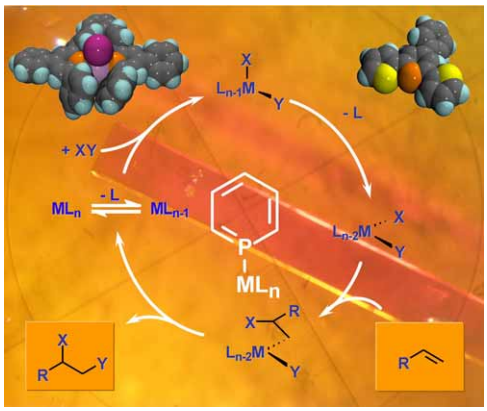

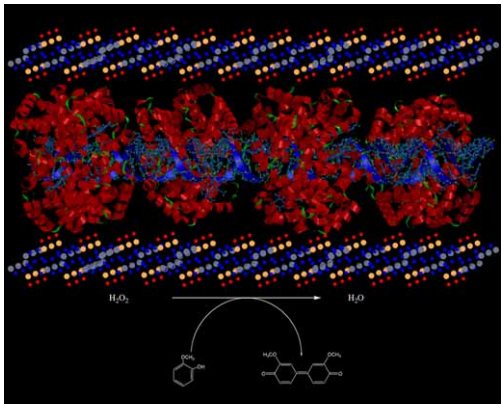

Images reproduced by permission of Christian Muller (outside) and Challa Kumar (inside)

Other papers published in this issue include:

Access to well-defined isolated Fe(II) centers on silica and their use in oxidation
Charbel Roukoss, Steven Fiddy, Aimery de Mallmann, Nuria Rendón, Jean-Marie Basset, Emile Kuntz and Christophe Copéret, *Dalton Trans.*, 2007, **DOI:** 10.1039/b711015d

Phosphinines as ligands in homogeneous catalysis: recent developments, concepts and perspectives
Christian Müller and Dieter Vogt, *Dalton Trans.*, 2007, **DOI:** 10.1039/b712456m

"Solventless" continuous flow homogeneous hydroformylation of 1-octene
Anja C. Frisch, Paul B. Webb, Guoying Zhao, Mark J. Muldoon, Peter J. Pogorzelec and David J. Cole-Hamilton, *Dalton Trans.*, 2007, **DOI:** 10.1039/b712683b

Palladium catalyzed Suzuki C–C couplings in an ionic liquid: nanoparticles responsible for the catalytic activity
Fernando Fernández, Beatriz Cordero, Jérôme Durand, Guillermo Muller, François Malbosc, Yolande Kihn, Emmanuelle Teuma and Montserrat Gómez, *Dalton Trans.*, 2007, **DOI:** 10.1039/b713449e

Visit the *Dalton Transactions* website for cutting-edge inorganic research

www.rsc.org/dalton

Evaluation of C_4 diphosphine ligands in rhodium catalysed methanol carbonylation under a syngas atmosphere: synthesis, structure, stability and reactivity of rhodium(I) carbonyl and rhodium(III) acetyl intermediates†

Gareth Lamb,[a] Matthew Clarke,*[a] Alexandra M. Z. Slawin,[a] Bruce Williams[b] and Lesley Key[b]

Received 23rd August 2007, Accepted 25th September 2007
First published as an Advance Article on the web 10th October 2007
DOI: 10.1039/b712974b

The carbonylation of methanol to acetic acid is a hugely important catalytic process, and there are considerable cost and environmental advantages if a process could be designed that was tolerant of hydrogen impurities in the CO feed gas, while eliminating by-products such as propionic acid and acetaldehyde altogether. This paper reports on an investigation into the application of rhodium complexes of several C_4 bridged diphosphines, namely BINAP, 1,4-bis(diphenylphosphino)butane (dppb), bis(diphenylphosphino)xylene (dppx) and 1,4-bis(dicyclohexylphosphino)butane (dcpb) as catalysts for hydrogen tolerant methanol carbonylation. An investigation into the structure, reactivity and stability of pre-catalysts and catalyst resting states of these complexes has also been carried out in order to understand the observations in catalysis. Rh(I) carbonyl halide complexes of each of the ligands have been prepared from both $[Rh_2(CO)_4Cl_2]$ and dimeric μ-Cl-$[Rh(L)Cl]_2$ complexes. These Rh(I) carbonyl complexes are either dimeric with bridging phosphine ligands (dppb, dcpb, dppx) or monomeric chelate complexes. The reaction of the complexes with methyl iodide at 140 °C has been studied, which has revealed clear differences in the stability of the corresponding Rh(III) complexes. Surprisingly, the dimeric Rh(I) carbonyls react cleanly with MeI with rearrangement of the diphosphine to a chelate co-ordination mode to give stable Rh(III) acetyl complexes. The Rh acetyls for L = dppb and dppx have been fully characterised by X-ray crystallography. During the catalytic studies, the more rigid dppx and BINAP ligands were found to be nearly 5 times more hydrogen tolerant than $[Rh(CO)_2I_2]^-$, as revealed by by-product analysis. The origin of this hydrogen tolerance is explained based on the differing reactivities of the Rh acetyls with hydrogen gas, and by considering the structure of the complexes.

Introduction

The carbonylation of methanol to acetic acid is one of the most important applications in homogeneous catalysis. Large scale industrial processes have typically used either $[Rh(CO)_2(I)_2]^-$ or $[Ir(CO)_2(I)_2]^-$ as catalysts with methyl iodide[1–3] and some ruthenium halide scavengers as promoters.[4–6] The current Cativa™ process uses an iridium catalyst with a high activity and selectivity towards acetic acid.

Phosphine-modified Rh catalysts have also received intense attention, with the main goal being to further increase activity and selectivity.[7–17] The commercial processes for carbonylation uses pure CO, which is purified from syngas (1 : 1 CO/H_2) in an energy intensive and expensive process. Propionic acid is the main liquid by-product requiring distillation to produce high grade acetic acid. A step change in methanol carbonylation technology would be to reduce propionic acid levels such that fractional distillation was not required, and/or to develop catalysts able to utilise lower grade CO that contains hydrogen. Most of the possible variables have now been explored in the 'unmodified' catalyst systems, and phosphine modified catalysts may offer the best opportunity for fine-tuning the selectivity of the catalysts.[18]

An extremely interesting paper by Moloy and Wegman in 1989 described reductive carbonylation of methanol with (2 : 1 H_2/CO) syngas to give ethanol and ethanal.[19,20] Good selectivities towards reductive carbonylation products were observed with C_3 diphosphines such as 1,3-bis(diphenylphosphino)propane (dppp). These authors also studied key organometallic intermediates in the dppp-based system to shed light on the basic mechanism. This paper notes that the C_4 diphosphine, 1,4-bis(diphenylphosphino)butane (dppb), was particularly ineffective for reductive carbonylation, predominantly giving acetic acid derivatives as products. The poor selectivities observed with the dppb catalysts in this application suggested that this type of phosphine could offer opportunities in hydrogen tolerant methanol carbonylation. In this paper, the synthesis and characterisation of rhodium complexes of C_4 diphosphines and their application in methanol carbonylation using syngas is reported.

Results and discussion

Coordination chemistry

The reaction of dppb with $[Rh(CO)_2Cl]_2$ has been reported to give the dimeric complex $[Rh(dppb)CO(Cl)]_2$, **1**.[21] **1** was prepared by

[a]*School of St. Andrews, University of St. Andrews, St. Andrews, Fife, UK KY16 9ST. E-mail: mc28@st-andrews.ac.uk; Fax: +44 (0)1334 463808; Tel: +44 (0)1334 463808*
[b]*BP Chemicals Ltd, Saltend, Hull, UK HU12 8DS*

† CCDC reference numbers 658319–658321. For crystallographic data in CIF or other electronic format see DOI: 10.1039/b712974b

the literature route, and our more extensive data agrees with the proposed formulation. In particular, FAB MS shows a M^+ 1184.1 peak as the highest mass ion and fragments assigned to $[M - Cl]^+$ (1149.1), and $[M - 2CO]^+$ (1128.1), that would seem unlikely to arise from monomeric or polymeric complexes.

The original report on the synthesis of $[Rh(dppb)CO(Cl)]_2$ **1**, notes that it is not clear if this complex with bridging bidentate diphosphine ligands is a kinetic or thermodynamic product. To investigate this further, $[Rh(dppb)Cl]_2$ **2**,[22] in which dppb acts as a chelate ligand, was treated with CO (Scheme 1). Quantitative formation of the bridging complex is observed: the fact that the dppb ligand rearranges from chelate to bridging ligand during the reaction with CO supports **1** being the thermodynamically preferred arrangement for this complex.

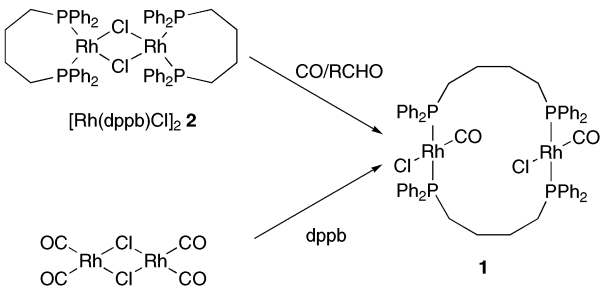

Scheme 1 Alternative methods for the formation of $[Rh(dppb)CO(Cl)]_2$.

The carbonylation of $[Rh(dppb)Cl]_2$ **2** by decarbonylation of aldehydes[23] was also investigated as an alternative route to rhodium–diphosphine carbonyl complexes. All of the alkyl and aryl aldehydes of varying electronic properties (fluorobenzaldehyde, 4-methoxybenzaldehyde, *etc.*) gave quantitative conversion of the Rh starting material to $[Rh(dppb)CO(Cl)]_2$ after 10 min at 120 °C. The bulky aldehyde 2-carboxymethyl-2′-methylpropionaldehyde[24] on the other hand gave a mixture of products.

Reactions of 1,4-bis(dicyclohexylphosphino)butane (dcpb) and bis(diphenylphosphino)xylene (dppx) with $[Rh(CO)_4Cl]_2$ also gave sparingly soluble dimeric complexes, **3** and **4** respectively with bridging bidentate phosphine ligands (Fig. 1).

In contrast, reaction of $[Rh(CO)_2Cl]_2$ with *rac*-BINAP or reaction of $[Rh(rac\text{-}BINAP)Cl]_2$[25] with CO gave the monomeric chelate complex, **5**.[26] This complex reacts with NaI in acetone to give the iodo analogue, **6** (Fig. 2). The structure of [Rh(*rac*-BINAP)(CO)I] was determined by X-ray crystallography.

Structurally [Rh(*rac*-BINAP)CO(I)] is quite typical of other Rh/BINAP complexes with respect to bond lengths and angles.[27,28] The expected *trans* influence of the CO is also seen, with the P(2)–Rh bond length (2.3769(12) Å) being significantly longer than that of the bond *trans* to the halide (2.2374(12) Å).

Investigating stability and reactivity of Rh(I) carbonyl complexes

The reactivity and stability of complexes **1** and **3–5**, in the presence of methyl iodide, was then examined. $[Rh(dppb)(CO)Cl]_2$ was previously reported to be unreactive with methyl iodide.[29] However, in our hands, heating **1** with MeI at 140 °C for 10 min in a glass pressure vessel in a microwave smoothly generates $[Rh(dppb)(C(O)CH_3)(I)_2]$ **7**, as the only phosphorus containing

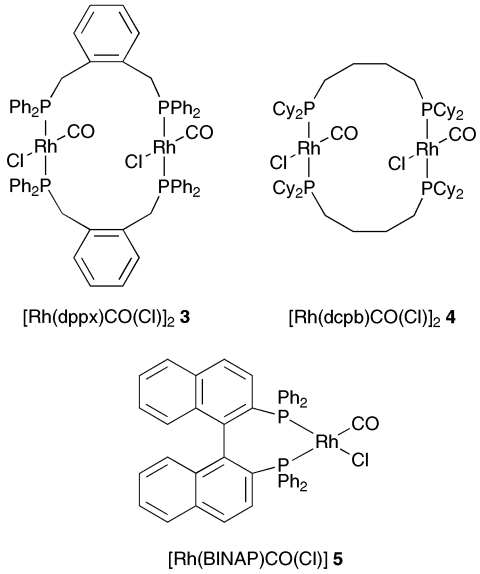

Fig. 1 Rhodium/C_4-phosphine complexes.

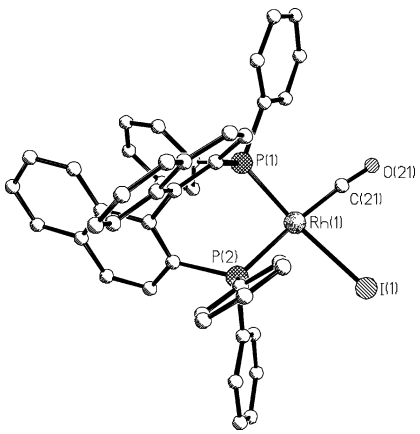

Fig. 2 X-Ray structure analysis of [Rh(BINAP)CO(I)] **6**.

product. The stability and reactivity of other carbonyl complexes including $[Rh(PPh_3)_2(CO)Cl]$ was then examined in greater detail. Stability was assessed by heating with a large excess of MeI (300 eq.) for an exact period of time (60 min) at a set temperature, followed by recording a ^{31}P NMR spectrum of an accurately measured aliquot (0.50 ml) relative to a calibrated external standard of $^nBu_3P{=}O$ (solution in C_6D_6 in a capillary tube). This study was complicated by the low solubility of some of the complexes, which precipitated from solution. The data reported in Table 1 therefore shows both the relative concentration of Rh phosphine species in solution and the % of the phosphorus species observed being the expected Rh–carbonyl or Rh–acetyl species. The differences between the ligands are quite striking.

The dppb and dppx carbonyl complexes react smoothly with MeI at 140 °C, and after 60 min of reaction time, only very small traces of anything other than the Rh–acetyl complexes are detectable in solution (entries 1 and 3). $[Rh(PPh_3)_2(CO)Cl]$ reacts with MeI at 60 °C, but after only 10 min at a temperature of 100 °C or above, extensive decomposition to $Ph_2P(O)OH$ and $Ph_3PMe^+I^-$ takes place. This is quantitative after 10 min at 140 °C. For dppb and dppx complexes, a higher temperature of 150 °C was needed

Table 1 Stability of Rh(I) carbonyl complexes in the absence of CO

Entry	Ligand	T/°C	% in solution[a]	% Rh–P species[b]
1	dppb	140	44.3	94.4
2	dppb	150	58.3	33.5
3	dppx	140	19.5	> 99
4	dppx	150	48.3	83.3
5	dcpb	140	0	0
6	BINAP	140	0	0
7	PPh_3	140	0	0

[a] % of complex remaining in solution relative to an external standard of tributylphosphine oxide calibrated against Rh starting material. [b] % of the NMR signals that can be attributed to Rh complexes relative to the singlets attributed to P(V) species.

to differentiate between their stability. At 150 °C dppb complexes start to decompose more readily resulting in only 33.5% stability whereas dppx complexes are able to maintain a greater stability even at this higher temperature.

The high stability of these complexes is somewhat surprising, since the dppb and dppx analogues have to rearrange from a bridging bidentate co-ordination mode to a monomeric chelate during the oxidative addition (or migratory insertion) process, and this presumably involves dissociation of one end of the diphosphine. This rearrangement must be fast relative to quaternisation of the phosphine. More surprising was the observation that despite many attempts, [Rh(*rac*-BINAP)(CO)Cl] reacts with MeI with severe decomposition: several phosphorus peaks without ^{31}P–Rh coupling are visible after 60 min at 140 °C. Thus in this case, a Rh(I) chelate complex shows lower stability than a Rh(I) bridging bidentate complex.

Rh(III) acetyls for dppb and dppx could be isolated by this preparative method in good yield. Using the rhodium acetonitrile complex $[Rh(NCMe)CO(I)_2COMe]_2$[30] it was hoped that the BINAP and dcpb acetyls could be synthesised. However, both reactions did not go cleanly producing a mixture of products. In the case of BINAP, the reaction most likely formed an acetyl species ($^{31}P\{^1H\}$ NMR (CD_2Cl_2): δ 32.6 (dd, $^1J_{Rh-P}$ 140.2 Hz, $^2J_{P-P}$ 14.9 Hz), 21.5 (dd, $^1J_{Rh-P}$ 138.1 Hz, $^2J_{P-P}$ 14.9 Hz); IR (KBr), ν(CO): 1706.9 cm^{-1}) and a set of minor signals ($^{31}P\{^1H\}$ NMR (CD_2Cl_2): δ 43.7 (dd, $^1J_{Rh-P}$ 161 Hz, $^2J_{P-P}$ 43.1 Hz), 21.5 (dd, $^1J_{Rh-P}$ 125.1 Hz, $^2J_{P-P}$ 43.1 Hz); IR (KBr), ν(CO): 2001 cm^{-1}) relating to the Rh(I) complex [Rh(*rac*-BINAP)CO(I)]. The formation of the latter product for BINAP in the absence of CO, presumably, by a reverse process of migration and reductive elimination of MeI may imply lower stability for the Rh(III) acetyl. In any case, there seems to be a stark difference in stability and reactivity of these C_4-diphosphine complexes.

Molecular structures of rhodium acetyl complexes

Crystals of [Rh(dppb)(C(O)CH_3)(I)$_2$] **7** and [Rh(dppx)(C(O)CH_3)-(I)$_2$] **8** suitable for X-ray diffraction could be grown by slowly blowing nitrogen over the reaction mixture. The structures of these complexes were then determined by X-ray crystallography (Fig. 3 and 4).

Going from a C_1 to a C_4 backbone it can be seen that Rh–P and C–O bond lengths steadily increase (Table 2). Bond angles are also affected with a P–Rh–P angle increasing from 73 to 103°, coupled with a decreasing I–Rh–I angle. Although there is little difference between the bond lengths of dppb and dppx complexes, the bond angles follow the previous trends of an increasing P–Rh–P and decreasing I–Rh–I angle.

Table 2 Comparison of X-ray data for [Rh(L)COMe(I)$_2$] complexes for C_1-, C_2-, C_3- and C_4-diphosphines

	Rh–P[a]/Å	C–O/Å	I–Rh–I/°	P–Rh–P/°
dppm[31]	2.265	1.160(3)	90.55(10)	73.30(2)
dppe[32]	2.276	1.178(9)	91.62(4)	84.74(7)
dppp[19]	2.288	1.182(7)	89.15(2)	90.49(5)
dppb **7**	2.312	1.196(4)	86.84(16)	99.13(3)
dppx **8**	2.309	1.210(13)	85.63(4)	103.31(11)

[a] Average bond length of Rh–P[1] and Rh–P[2].

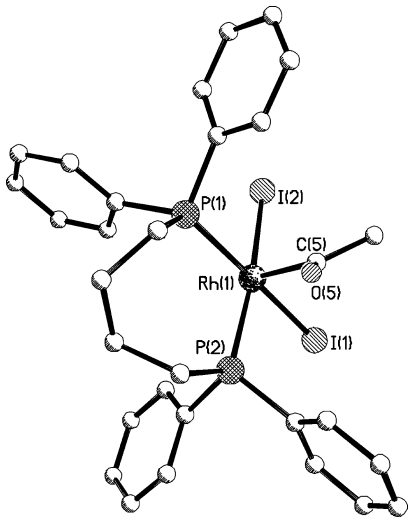

Fig. 3 Molecular structure of [Rh(dppb)(COMe)(I)$_2$] **7**.

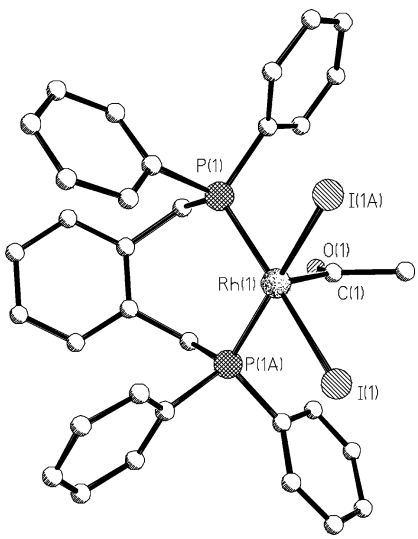

Fig. 4 Molecular structure of [Rh(dppx)(COMe)(I)$_2$] **8** with a mirror plane at (x, $-y + 0.5$, z) bisecting the molecule.

With a greater understanding of Rh co-ordination chemistry of the C_4 ligands in hand, we undertook catalytic studies in carbonylation of methanol using CO/H_2 mixtures.

Methanol carbonylation

Several carbonylation reactions were run under differing conditions. Our main aim was to compare a range of C_4 ligands in a series of *in situ* experiments and come up with a rational design for a hydrogen tolerant system for methanol carbonylation (Scheme 2).

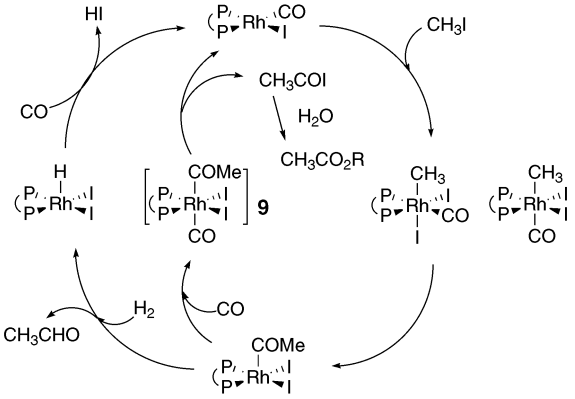

Scheme 2 Postulated mechanism for carbonylation *versus* reductive carbonylation in a rhodium–diphosphine–methyl iodide catalysed reaction.

The catalytic cycle shown in Scheme 2 demonstrates the competing reactions. When hydrogen is present acetaldehyde may be formed *via* the pathway on the left hand side of the cycle. However, this must compete with the carbonylation reaction forming the reactive intermediate **9** from which several carbonylated products are possible depending on the water concentration of the system.

Therefore several carbonylation reactions were run using different gas mixtures and water concentrations. At 100 °C 22.6 g of MeI was charged into 100 g of methanol containing the precursor $Rh_2CO_4Cl_2$ and the phosphine ligand. The solution was then heated at 140 °C for 40 min under a pressure of 26 bar of CO and after the reaction was complete both liquid and gas samples were taken for analysis.

The results highlighted in bold, in Tables 3 and 4, comprise the most significant data. These being the amount of desired products formed *i.e.* acetic acid and methyl acetate, the amount of acetaldehyde produced, as well as the gaseous side-product methane.

By looking at the amount of methyl acetate and acetic acid produced we can start to build up a picture of the activity of these systems and what affect the phosphine ligand has upon this. The dppb system at 140 °C appears to be the most active (965 TOF/h^{-1}) followed by the non-modified system (581 TOF/h^{-1}). The least reactive under these conditions were the dppx and the BINAP systems.

The primary liquid by-product was acetaldehyde, under an atmosphere of CO we would expect to see very little produced and this is what is observed. By running the reactions using 5 : 1 CO/H_2 gas mixtures at 150 °C with 15% H_2O the hydrogen tolerance of these systems was evaluated.

The order of reactivity for the catalysts was dppb> $Rh_2CO_4Cl_2$>dcpb>BINAP>dppx. The dppb system proved to be the most active with $Rh_2CO_4Cl_2$ and the dcpb systems also showing high activity relative to the dppx and BINAP systems, that were approximately 50% less active.

The greatest change in the products compared with the previous experiment was the increase in the by-product acetaldehyde which increased by as much as 35 times in the case of $Rh_2CO_4Cl_2$ and dppb. Both Tables 3 and 4 show the mol% of acetaldehyde/carbonylation products, from these calculations it can be seen that the dppx system is 4.5 times as hydrogen tolerant as $[Rh(CO)_2I_2]^-$ with as little as 0.74% of the carbonylated products being the undesired by-product acetaldehyde.

As well as acetaldehyde both the dppb and dcpb systems formed large amounts of methane, in the case of the dppb system >25% of the autoclave headspace was methane, whereas dppx and BINAP systems gave very little methane as a gaseous by-product with BINAP giving <0.1 %vol vol^{-1}.

In conclusion, dppx and BINAP systems although suffering from comparably low activity are very hydrogen tolerant producing between 135–185 ppm of acetaldehyde at 150 °C and almost neglible amounts of methane in all catalytic experiments. To the best of our knowledge the dppx system is the most hydrogen tolerant catalyst for the rhodium catalysed carbonylation of methanol reported to date.[18]

Table 3 Methanol carbonylation using pure CO[a]

Ligand	None	dppb	dppx	dcpb	BINAP
TOF[b]/h^{-1}	581	965	208	465	174
Aldehyde/acetyl ratio[c]	0.085	0.046	0.080	0.031	<0.079
Liquid analysis[d]/%mol mol^{-1}					
Water	14.4	17.6	12.3	14.7	11.9
Methanol[e]	78.5	73.1	82.9	78.9	83.7
Methyl iodide	3.0	2.8	3.3	3.2	3.2
Methyl acetate	3.9	6.2	1.4	3.1	1.2
Acetic acid	0.2	0.4	0.1	0.1	0.1
MeCHO (ppm)	35	30	12	10	<10
Gas analysis[f]/%vol vol^{-1}					
H_2	0.6	<0.1	<0.1	4.9	<0.1
CO	82.5	86.9	85.8	84.2	89.0
CO_2	0.2	0.09	<0.1	<0.02	0.04
CH_4	0.4	0.08	<0.1	0.4	<0.05

[a] Reaction conditions: $Rh_2CO_4Cl_2$ (0.386 mmol), Rh : ligand = 1 : 1, CO p = 26 bar, for 40 min at 140 °C. [b] TOF was calculated from the total conversion of methanol and methyl iodide to methyl acetate and acetic acid. [c] Aldehyde/acetyl ratio was calculated from the ratio of acetaldehyde to carbonylated products. [d] Calculated by calibrated GC analysis using an internal standard at BP, Hull. [e] %mol mol^{-1} of methanol also comprises ~5–7 %mol mol^{-1} DME. [f] Sampled at room temperature from headspace after cool down.

Table 4 Methanol carbonylation at 150 °C, 15% H_2O and 5 : 1 CO : H_2[a]

Ligand	None	dppb	dppx	dcpb	BINAP
TOF[b]/h^{-1}	740	857	387	690	426
Aldehyde/acetyl ratio[c]	3.20	2.59	0.74	2.30	0.92
Liquids analysis[d]/%mol mol^{-1}					
Water	45.4	44.5	42.9	43.9	43.5
Methanol[e]	49.8	50.2	53.8	51.3	53.0
Methyl iodide	1.5	1.4	1.5	1.6	1.6
Methyl acetate	2.7	3.2	1.5	2.6	1.7
Acetic acid	0.6	0.7	0.3	0.6	0.3
MeCHO (ppm)	1100	1040	135	750	185
Gas analysis[f]/%vol vol^{-1}					
H_2	37.2	27	27.0	31.4	20.2
CO	44.4	43.6	69.6	42.1	78.2
CO_2	2.3	1.8	0.5	1.1	0.3
CH_4[g]	14.4	25.8	1.7	23.9	<0.1

[a] Reaction conditions: $Rh_2CO_4Cl_2$ (0.386 mmol), Rh : ligand = 1 : 1, CO/H_2 = 5 : 1, p = 26 bar, for 40 min at 150 °C with an initial water concentration of 15%. [b] TOF was calculated from the total conversion of methanol and methyl iodide to methyl acetate and acetic acid. [c] Aldehyde/acetyl ratio was calculated from the ratio of acetaldehyde to carbonylated products. [d] Calculated by calibrated GC analysis using an internal standard at BP, Hull. [e] %mol mol^{-1} of methanol also comprises 5–7 %mol mol^{-1} DME. [f] Sampled at room temperature from headspace after cool down. [g] %vol vol^{-1} of methane typically represent between 0.0001–0.6 %mol mol^{-1} converted from the initial %mol mol^{-1} of methanol and MeI.

Table 5 % of catalyst recovered under different syngas conditions

	2 : 1 H_2 : CO 140 °C, 40 min	5 : 1 H_2 : CO 150 °C, 40 min
dppb	60.2	2.7
dppx	85	78.7
dcpb	27.8	5.9
BINAP	63.9	53.8

Catalyst resting states and catalyst stability

On cooling, the catalysts precipitated out of solution. It should be noted that the % recovery of precipitated catalyst does not completely decouple stability from solubility differences so the results contained in Table 5 must be interpreted cautiously. However, since all the Rh complexes involved show very limited solubility in the product mix it is very likely that these reflect catalyst stability. The precipitate collected from the BINAP systems was shown to be the Rh(I) carbonyl iodide species [Rh(BINAP)CO(I)]. Although HPIR studies during the reaction were inconclusive, given that we also observed a lower stability of BINAP Rh(III) acetyls in the coordination studies, [Rh(BINAP)(CO)I] is the proposed resting state. The higher stability of the BINAP catalyst under catalytic conditions can be ascribed to the presence of CO which enables the system to turnover and produce a Rh(I) resting state.

The Rh/dcpb catalyst that precipitated was only sparingly soluble with the ^{31}P NMR showing the presence of a Rh(III) species with a typical P–Rh coupling of 138 Hz. However, FT-IR of the bulk sample showed that the majority to be the Rh(I) species [Rh(dcpb)CO(I)] (1949 cm^{-1}) with a minor peak at 1710 cm^{-1} relating to the acetyl. Therefore, it is likely that the nature of the catalyst resting state is finely balanced. However, it is noted that the recovery of these sparingly soluble species was relatively low.

One may possibly expect the dcpb system to be much more active than dppb due to the strongly electron donating properties of the phosphines which may facilitate oxidative addition, with the bulky groups favouring reductive elimination. However, a reasonable explanation for similar performance is the increase in steric hindrance of the cyclohexyl groups and the considerable shielding these must give to the metal centre. Alternatively, given that we have been unable to isolate Rh species for dcpb in stoichiometric reactions and much lower recovery at the end of the catalytic runs had occurred, it is also possible that dcpb catalysts decompose under the reaction conditions.

For dppx and dppb on the other hand, it was possible to collect a substantial amount of precipitate formed at the end of each catalytic run. These precipitates were fully analysed and the resting state shown to be the Rh(III) species, [Rh(L)(C(O)Me)$(I)_2$]. The most stable catalyst system is dppx which manages 85% recovery as a precipitate under catalytic conditions at 140 °C, and was also seen to be the most stable in the previous study in hot MeI. In the runs carried out in aqueous methanol at 150 °C, a similar crop of [Rh(dppx)(C(O)Me)$(I)_2$] was obtained (79%) in comparison to the dppb catalyst that provided very little of the Rh acetyl precipitate. This is most likely due to decomposition of dppb complexes at higher temperatures.

Reaction of dppp, dppb and dppx complexes with hydrogen

The greater hydrogen tolerance of the dppx catalyst could reflect a more efficient migratory insertion/reductive elimination for this ligand, or a reduced propensity for the complexes to undergo hydrogenolysis. According to Moloy and Wegman it is possible to generate the hydride dimer and acetaldehyde (as dimethyl acetal) by reacting [Rh(dppp)(C(O)Me)$(I)_2$] with hydrogen (Scheme 3).[20] We have investigated ligand effects on this by reacting the isolated acetyls [Rh(dppp)(C(O)Me)$(I)_2$], [Rh(dppb)(C(O)Me)$(I)_2$] and [Rh(dppx)(C(O)Me)$(I)_2$] with hydrogen under similar conditions set out above.

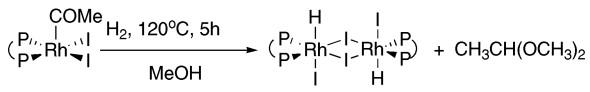

Scheme 3 Reaction of [Rh(dppp)COMe$(I)_2$] with H_2 and the formation of the hydride dimer.

[Rh(dppp)(C(O)Me)(I)$_2$] was heated at 120 °C for 5 h under 7 bar of H_2, this yielded a complex with the same spectroscopic data as previously described for the hydride dimer (^{31}P NMR δ 27.3, d, J_{Rh-P} = 125 Hz). Under these conditions we also observed the hydrogenolysis of [Rh(dppb)(C(O)Me)(I)$_2$] and the formation of several new complexes that show hydride signals in the ^{1}H NMR. Unfortunately we were unable to recover this new complex in an analytically pure form. Interestingly, when [Rh(dppx)(C(O)Me)(I)$_2$] was reacted under the same forcing conditions no reaction occurred and the starting material was recovered in quantitative yield.

When this experiment was repeated at the lower temperature of 80 °C the complexes containing dppp and dppb react to form Rh–hydrides. However, [Rh(dppx)(C(O)Me)(I)$_2$] once again does not react with hydrogen and in fact at the lower temperature it starts to equilibrate back to the Rh(I) species [Rh(dppx)CO(I)]. This is backed up by both ^{31}P NMR data as well as FT-IR of the mixture, that clearly shows peaks for both the acetyl and the Rh(I) carbonyl. Interestingly, the [Rh(dppx)CO(I)] being formed by this reverse process is a monomeric chelate species as opposed to a dimeric bridging species formed from $Rh_2CO_4Cl_2$. There is therefore a clear difference in the reactivity of the Rh(III) acetyls with hydrogen that co-incides with the observations under catalytic conditions.

One possible explanation for hydrogen tolerance can be seen when the crystal structures of the dppb and dppx acetyls are compared. The more rigid dppx backbone forces the phenyl groups inwards increasing the steric hindrance around the Rh–acetyl bond. It seems reasonable that this more congested environment around the metal centre coupled with the fact that dppx cannot easily change conformation to accommodate incoming reactants, accounts for the differences in catalytic products.

Conclusion

In summary, Rh(I) carbonyl complexes of the C_4-diphosphines dppb, BINAP, dcypb and dppx have been prepared and their reactivity studied. These studies reveal that only the dppb and dppx complexes smoothly give the expected Rh(III) acetyl complexes on reaction with a large excess of methyl iodide at 140 °C. The complexes have been studied as catalysts for methanol carbonylation using CO that contains hydrogen. Examination of the insoluble catalyst residues from these reactions shows that dppx and dppb have Rh(III) acetyls as resting states and that the dppx complex is more stable with respect to elimination of P(V) by-products. In contrast, the dcpb system consisted of both Rh(I) carbonyl and Rh(III) acetyl species. By-product analysis of the organic carbonylation products reveals that the more rigid BINAP and dppx systems give much lower proportions of acetaldehyde and methane side products. An explanation for this comes from the relative reactivity of the Rh(III) acetyls with hydrogen: whereas dppb and dppp react with hydrogen to give various hydride species, there is no reaction for the dppx complex. Examination of the X-ray crystal structures of these two complexes suggest that the rigidity of the dppx backbone makes the diphenylphosphine group shield the acetyl from hydrogenolysis, which may be the ultimate origin of the greater hydrogen tolerance of the dppx carbonylation catalysts. Further studies to gain a greater understanding of the stability and hydrogen tolerance of phosphine modified rhodium carbonylation catalysts are ongoing.

Experimental

General

All manipulations were performed using standard Schlenk line techniques under nitrogen supplied by BOC. All chemicals and solvents were obtained through commercial sources. All complexes used were prepared by standard literature procedures. Microanalyses were by the University of St. Andrews microanalytical service. NMR spectra were recorded on Bruker Advance 300 instruments. Chemical shifts are reported in ppm with ^{1}H and ^{13}C NMR spectra referenced to tetramethylsilane (external). ^{31}P NMR spectra were referenced externally to 85% H_3PO_4. Proton and carbon signal multiplicities are given as s (singlet), d (doublet), t (triplet), q (quartet), m (multiplet), b (broad) or a combination of these. All spectra were recorded at room temperature and the solvent for a particular spectrum is given in parentheses. ^{13}C and ^{31}P NMR spectra were recorded with broad band proton decoupling. IR spectra were recorded using a Perkin Elmer Spectrum GX FT-IR system. All solids were analysed as KBr disks. Gas chromatography was carried out at BP PLC, Saltend. Mass spectroscopy data were obtained from the EPSRC National Mass Spectroscopy Service Centre, Swansea. In addition to detecting the ions shown, all Rh complexes showed excellent agreement between calculated and expected isotope patterns.

Catalysis experiments

These experiments were carried out at BP chemicals Ltd in Hull in a 300 cm^3 Hastelloy high pressure infrared (HPIR) autoclave fitted with a bursting disc, catalyst injector, overhead Magnedrive™ stirrer, impeller with gas sparging facility, gas inlet, high pressure (195 bar) carbon monoxide reservoir and thermocouple. Additionally the apparatus featured equipment for pressure measurements and sampling. Carbon monoxide consumption was measured by monitoring the pressure drop in the reservoir. A computer collected the data automatically by use of a Dynamic Data Exchange (DDE) ink between an Orsi process control package and a data logging package on Excel.

CAUTION: These experiments were carried out using custom made facilities dedicated to methanol carbonylation. MeI and CO are extremely toxic and should be used with extreme care.

For the reactions carried out with an initial water level of 15% w/w, methanol (100 g, 3.125 mol), water (19 g, 1.06 mol), $Rh_2CO_4Cl_2$ (150 mg, 0.386 mmol) and diphosphine ligand (2 eq, 0.772 mmol) were added to the autoclave under CO/syngas. The quantity of water was altered for the remaining reactions incorporating no initial water content. The autoclave was then sealed and pressurised with carbon monoxide (5 bar) and heated to 100 °C, controlled by the use of a thermocouple in a thermowell in the reaction solution, whilst stirring at 900 rpm. Using the catalyst injector iodomethane (22.6 g, 0.159 mol) was then added to the autoclave with an over pressure of CO/syngas. Simultaneously, the autoclave was pressurised with CO/syngas (27 bar) from the high pressure ballast vessel. The autoclave was then heated to the desired temperature and the data collection activated. The

pressure was maintained at 27 bar by a pressure regulating value which transferred CO/syngas from the high pressure ballast to the autoclave when the pressure dropped below the set-point.

After the reaction, the autoclave was allowed to cool before a gas sample was collected from the headspace in the autoclave. This gas sample was analysed by gas chromatography using in-house facilities.

The autoclave was then disconnected from the kinetics rig and a liquid sample of the reaction solution was analysed by gas chromatography. Liquid analysis was carried out for the main constituents, that fall into the bulk liquids category, as well as a range of liquid by-products such as acetaldehyde.

X-Ray crystallography

X-Ray crystallography data were collected at 93 K by using a Rigaku MM007 High Brilliance RA generator and Mercury/Saturn CCD systems using Mo-K_α radiation. Intensities were corrected for Lorentz-polarisation and for absorption. The structures were solved by direct methods. All hydrogen atoms were refined as idealised riding geometries and structural refinements were obtained with full-matrix least-squares based on F^2 by using the program SHELXTL.

Crystal structure determination.

Crystal data for [Rh(BINAP)(CO)I]. $C_{45}H_{32}IOP_2Rh$, M = 880.46, triclinic, a = 11.1576(12), b = 11.5084(16), c = 14.6153(15) Å, α = 84.203(7)°, β = 71.704(7)°, γ = 89.593(10)°, V = 1772.1(4) Å^3, T = 93(2) K, space group $P\bar{1}$, Z = 2, 11 550 reflections measured, 6105 unique of which 4758 were observed [$I < 2\sigma I$] (R_1 = 0.0474, wR_2 = 0.0865, R_{int} = 0.0409).

Crystal data for [Rh(dppb)(COMe)I$_2$]. $C_{30}H_{31}I_2OP_2Rh\cdot[C_3H_6O_2]0.5$, M = 863.24, monoclinic, a = 21.540(4), b = 8.1514(14), c = 18.908(4) Å, β = 96.662(3)°, V = 3297.5(11) Å^3, T = 93(2) K, space group $P2(1)/c$, Z = 4, 22 888 reflections measured, 5963 unique of which 5162 were observed [$I < 2\sigma I$] (R_1 = 0.0258, wR_2 = 0.0519, R_{int} = 0.0310).

Crystal data for [Rh(dppx)(COMe)I$_2$]. $C_{34}H_{31}I_2OP_2Rh\cdot CHCl_3$, M = 993.61, orthorhombic, a = 24.241(4), b = 18.209(3), c = 8.1431(14) Å, V = 3594.5(11) Å^3, T = 93(2) K, space group *Pnma*, Z = 4, 21819 reflections measured, 3338 unique of which 2388 were observed [$I < 2\sigma I$] (R_1 = 0.0641, wR_2 = 0.1305, R_{int} = 0.1380).

General synthesis of [Rh(L)CO(Cl)]$_2$

Method A. THF (2 cm^3) was charged into a Schlenk tube containing the diphosphine (2 eq.) and the precursor $Rh_2CO_4Cl_2$. After stirring for a short amount of time a pale yellow solid precipitated which was filtered off and washed with ice cold methanol before drying under vacuum. Yields quoted below are all using method A.

Method B. THF (2 cm^3) was charged into a Schlenk tube containing the diphosphine (2 eq.) and the precursor [Rh(cyclooctene)Cl]$_2$. CO was then bubbled through the solution resulting in a pale yellow solid which was washed with ice cold methanol before drying under vacuum.

Method C. THF (1.5 cm^3) was charged into a microwave vial containing the diphosphine (2 eq.) and the precursor [Rh(coe)Cl]$_2$. This was stirred for 10 min before adding the aldehyde (100 eq.) in THF (0.5 cm^3). The solution was then heated at 110 °C for 10 min in a Biotage™ microwave and the resulting yellow solution was then analysed.

Note: Several of these complexes were too insoluble to record meaningful ^{13}C NMR data.

Synthesis of [Rh(dppb)CO(Cl)]$_2$[29]. Yield: 90% (136.8 mg, 0.116 mmol); IR (KBr), ν(CO)/cm^{-1}: 1959.6. LSIMS Found 1184.2 M$^+$; $C_{58}H_{56}Cl_2O_2P_4Rh_2$ requires 1184.1 M$^+$. ^{31}P{^{1}H} NMR (CD_2Cl_2): δ 24.0 (d, $^1J_{Rh-P}$ 124 Hz).

Synthesis of [Rh(BINAP)CO(Cl)][25]. Yield: 79% (95.6 mg, 0.121 mmol). IR (KBr), ν(CO)/cm^{-1}: 2007.1. LSIMS (FAB) Found 760.1 [M − CO]$^+$; $C_{44}H_{32}Cl_1P_2Rh_1$ requires 760.1 [M − CO]$^+$. ^{31}P{^{1}H} NMR (CD_2Cl_2): δ 46.8 (dd, $^1J_{Rh-P}$ 161.1 Hz, δ 25.0 (dd, $^1J_{Rh-P}$ 127.7 Hz).

Synthesis of [Rh(dppx)CO(Cl)]$_2$. Yield: 79.3% (48.4 mg, 0.041 mmol). IR (KBr), ν(CO)/cm^{-1}: 1970.3. LSIMS (FAB) Found 1224.1 [M − 2CO]$^+$, 1245.2 [M − Cl]$^+$; $C_{64}H_{56}Cl_2P_4Rh_2$ requires 1224.1 [M − 2CO]$^+$. ^{31}P{^{1}H} NMR (CD_2Cl_2): δ 30.7 (d, $^1J_{Rh-P}$ 127.7 Hz). ^{1}H NMR (CD_2Cl_2): δ_H 8.00–6.00 (28H, m), 3.85 (1H, s), 3.60 (1H, s), 2.95 (2H, s), 1.42 (2H, s), 1.25 (1H, s), 1.20 (1H, s).

Synthesis of [Rh(dcpb)CO(Cl)]$_2$. Yield: 74% (117 mg, 0.095 mmol). IR (KBr), ν(CO)/cm^{-1}: 1949.4. LSIMS (FAB) Found 1232.3 M$^+$; $C_{58}H_{104}Cl_2O_2P_4Rh_2$ requires 1232.4 M$^+$. Anal. calc. for $C_{58}H_{104}Cl_2O_2P_4Rh_2$: C, 56.45; H, 8.49%. Found: 56.22; H, 8.20%. ^{31}P{^{1}H} NMR (CD_2Cl_2): δ 31.5 (d, $^1J_{Rh-P}$ 118.8 Hz). ^{1}H NMR (CD_2Cl_2): δ_H 1.99 (16H, bm), 1.74 (48H, bm), 1.46 (16H, bm), 1.188 (16H, bm).

Synthesis of [Rh(BINAP)CO(I)]

Acetone (5 ml) was added to a Schlenk tube containing [Rh(BINAP)CO(Cl)] (50 mg, 0.063 mmol) and NaI (1.9 eq.). This resulted in a colour change from a yellow to an orange solution which was filtered and dried under vacuum to give the iodo-complex [Rh(BINAP)CO(I)]. Yield: 96% (53.6 mg, 0.061 mmol). (IR (KBr), ν(CO)/cm^{-1}: 2007.2. LSIMS (FAB) Found 851.9 [M − CO]$^+$; $C_{44}H_{32}IP_2Rh$ requires 852.0 [M − CO]$^+$. ^{31}P{^{1}H} NMR (CD_2Cl_2): δ 42.9 (dd, $^1J_{Rh-P}$ 166 Hz, $^2J_{P-P}$ 42.3 Hz), 21.9 (dd, $^1J_{Rh-P}$ 126 Hz, $^2J_{P-P}$ 42.3 Hz). This compound was further characterised by X-ray crystallography.

Synthesis of [Rh(dppb)(C(O)Me)(I)$_2$][30]

1.5 ml methyl acetate and 0.5 ml methyl iodide was added to a 2.0 ml Biotage™ microwave vial containing [Rh(dppb)CO(Cl)]$_2$ (15 mg, 0.013 mmol). The reaction mixture was then heated to 140 °C for 10 min. High quality X-ray crystals were then formed from the slow evaporation of this solution. Yield: 86% (17.8 mg, 0.022 mmol). IR (KBr), ν(CO)/cm^{-1}: 1701.8. LSIMS (FAB) Found 825.8 M$^+$; $C_{30}H_{31}I_2OP_2Rh$ requires 825.9 M$^+$. Anal. calc. for $C_{30}H_{31}I_2OP_2Rh$: C, 43.61; H, 3.78%. Found: C, 44.06; H, 3.76%. ^{31}P{^{1}H} NMR (CD_2Cl_2): δ 32.9 (d, $^1J_{Rh-P}$ 138.1 Hz. ^{1}H NMR (CD_2Cl_2): δ_H 7.58 (4H, C*H*-Ar, dt), 7.23–7.41 (12H, C*H*-Ar, m), 3.19 (2H, CH_2, m), 2.58 (3H, COCH_3, s), 2.35 (2H, CH_2, m), 1.49 (2H, CH_2, m), 0.98 (2H, CH_2, m). ^{13}C NMR (CD_2Cl_2): δ 212.85 (*C*OMe, dt, $^1J_{Rh-C}$ 25.77 Hz), 137.27, 136.54, 130.09, 130.27

(*C*-Ar), 136.44–127.30 (*C*H-Ar), 44.85 (*C*H_2, s), 23.53 (CH_2, d, $^1J_{Rh-C}$ 28.64 Hz), 21.46 (*C*H_3, s).

Synthesis of [Rh(dppx)(C(O)Me)(I)$_2$]

1.5 ml methyl acetate and 0.5 ml methyl iodide was added to a 2.0 ml Biotage™ microwave vial containing [Rh(dppx)CO(Cl)]$_2$ (15 mg, 0.012 mmol). The reaction mixture was then heated to 140 °C for 10 min. High quality X-ray crystals were then formed from the slow evaporation of this solution. Yield: 78.5% (56.0 mg, 0.064 mmol). IR (KBr), ν(CO)/cm^{-1}: 1710.6. LSIMS (FAB) Found 873.8 M$^+$, 746.9 [M − I]$^+$. $C_{34}H_{31}I_2OP_2Rh$ requires 873.9 M$^+$. Anal. calc. for $C_{34}H_{31}I_2OP_2Rh$: C, 46.71; H, 3.57%. Found: C, 46.56; H, 3.31%. $^{31}P\{^1H\}$ NMR (CD_2Cl_2): δ 11.0 (d, $^1J_{Rh-P}$ 138.7 Hz). ^{1}H NMR (CD_2Cl_2): δ_H 7.86 (4H, C*H*, dt), 7.23–7.45 (12H, C*H*, m), 6.43 (4H, CH_2, m), 6.09 (2H, CH_2, m), 5.02 (2H, CH_2, m), 3.34 (2H, CH_2, m), 2.38 (3H, CH_3, s).

Acknowledgements

We would like to thank Glenn Sunley for many fruitful discussions. EPSRC and BP for an industrial CASE studentship, EPSRC National Mass Spectroscopy Service, Caroline Horsborough from St. Andrews MS, Melanya Smith and Thomas Lebel from the NMR services department at the University of St. Andrews.

References

1 F. E. Paulik and J. F. Roth, *Chem. Commun. (London)*, 1968, 1578.
2 A. Haynes, P. M. Maitlis, G. E. Morris, G. J. Sunley, H. Adams, P. W. Badger, C. M. Bowers, D. B. Cook, P. I. P. Elliott, T. Ghaffar, H. Green, T. R. Griffin, M. Payne, J. M. Pearson, M. J. Taylor, P. W. Vickers and R. J. Watt, *J. Am. Chem. Soc.*, 2004, **126**, 2847.
3 G. J. Sunley and D. J. Watson, *Catal. Today*, 2000, **58**, 293.
4 A. Haynes, D. J. Law, A. Miller, G. E. Morris, M. J. Payne and J. G. Sunley, in Carbonylation catalyst and process for the production of acetic acid from methanol, *Br. Pat.*, WO 2005009939, 2005.
5 L. A. Key, M. J. Payne and A. D. Poole, in Catalytic carbonylation process for the production of acetic acid from methanol and carbon monoxide, *Br. Pat.*, 2004026805, 2004.
6 J. G. Sunley, in Manufacture of acetic acid by the iridium-catalyzed carbonylation using one or more metal iodides or iodide-generating salts or complexes, *Br. Pat.*, GB 2003–16681, 2003.
7 M. J. Baker, M. F. Giles, A. G. Orpen, M. J. Taylor and R. J. Watt, *J. Chem. Soc., Chem. Commun.*, 1995, 197.
8 C.-A. Carraz, A. G. Orpen, D. D. Ellis, P. G. Pringle, E. J. Ditzel and G. J. Sunley, *Chem. Commun.*, 2000, 1277.
9 J. R. Dilworth, J. R. Miller, N. Wheatley, M. J. Baker and J. G. Sunley, *J. Chem. Soc., Chem. Commun.*, 1995, 1579.
10 D. K. Dutta, J. D. Woollins, A. M. Z. Slawin, D. Konwar, P. Das, M. Sharma, P. Bhattacharyya and S. M. Aucott, *Dalton Trans.*, 2003, 2674.
11 P. M. Maitlis, A. Haynes, G. J. Sunley and M. J. Howard, *J. Chem. Soc., Dalton Trans.*, 1996, 2187.
12 J. Rankin, A. C. Benyei, A. D. Poole and D. J. Cole-Hamilton, *J. Chem. Soc., Dalton Trans.*, 1999, 3771.
13 J. Rankin, A. D. Poole, A. C. Benyei and D. J. Cole-Hamilton, *Chem. Commun.*, 1997, 1835.
14 Z. Freixa, P. C. J. Kamer, M. Lutz, A. L. Spek and P. W. N. M. van Leeuwen, *Angew. Chem., Int. Ed.*, 2005, **44**, 4385.
15 C. M. Thomas, R. Mafua, B. Therrien, E. Rusanov, H. Stoeckli-Evans and G. Suss-Fink, *Chem.–Eur. J.*, 2002, **8**, 3343.
16 C. M. Thomas and G. Suss-Fink, *Coord. Chem. Rev.*, 2003, **243**, 125.
17 S. Burger, B. Therrien and G. Suess-Fink, *Helv. Chim. Acta*, 2005, **88**, 478.
18 S. Gaemers and J. G. Sunley, in Carbonylation process using metal-polydentate ligand catalysts, *Pat. Appl.*, WO 2004101487, 2004.
19 K. G. Moloy and J. L. Petersen, *Organometallics*, 1995, **14**, 2931.
20 K. G. Moloy and R. W. Wegman, *Organometallics*, 1989, **8**, 2883.
21 A. R. Sanger, *J. Chem. Soc., Chem. Commun.*, 1975, 893.
22 J. A. Osborn and G. Wilkinson, *Inorg. Synth.*, 1967, **10**, 67.
23 D. Evans, J. A. Osborn and G. Wilkinson, *Inorg. Synth.*, 1968, **11**, 99.
24 M. L. Clarke and G. J. Roff, *Chem.–Eur. J.*, 2006, **12**, 7978.
25 K. A. Bunten, D. H. Farrar, A. J. Poe and A. Lough, *Organometallics*, 2002, **21**, 3344.
26 S. Jeulin, S. Duprat de Paule, V. Ratovelomanana-Vidal, J.-P. Genet, N. Champion and P. Dellis, *Angew. Chem., Int. Ed.*, 2004, **43**, 320.
27 K. Toriumi, T. Ito, H. Takaya, T. Souchi and R. Noyori, *Acta Crystallogr., Sect. B*, 1982, **38**, 807.
28 T. K. Hollis, L.-S. Wang and F. Tham, *J. Am. Chem. Soc.*, 2000, **122**, 11737.
29 A. R. Sanger, *J. Chem. Soc., Dalton Trans.*, 1977, 120.
30 A. Haynes, P. M. Maitlis, I. A. Stanbridge, S. Haak, J. M. Pearson, H. Adams and N. A. Bailey, *Inorg. Chim. Acta*, 2004, **357**, 3027.
31 H. Adams, N. A. Bailey, B. E. Mann and C. P. Manuel, *Inorg. Chim. Acta*, 1992, **198–200**, 111.
32 L. Gonsalvi, H. Adams, G. J. Sunley, E. Ditzel and A. Haynes, *J. Am. Chem. Soc.*, 2002, **124**, 13.